

The Antibacterial Cell Division Inhibitor PC190723 Is an FtsZ Polymer-stabilizing Agent That Induces Filament Assembly and Condensation^{*[5]}

Received for publication, December 21, 2009, and in revised form, February 18, 2010. Published, JBC Papers in Press, March 8, 2010, DOI 10.1074/jbc.M109.094722

José M. Andreu^{†1}, Claudia Schaffner-Barbero[‡], Sonia Huecas[‡], Dulce Alonso[§], María L. Lopez-Rodriguez[§], Laura B. Ruiz-Avila[‡], Rafael Núñez-Ramírez^{‡2}, Oscar Llorca[‡], and Antonio J. Martín-Galiano[‡]

From the [‡]Centro de Investigaciones Biológicas, Consejo Superior de Investigaciones Científicas, Ramiro de Maeztu 9 and

[§]Departamento de Química Orgánica, Facultad de Ciencias Químicas, Universidad Complutense Madrid, 28040 Madrid, Spain

Cell division protein FtsZ can form single-stranded filaments with a cooperative behavior by self-switching assembly. Subsequent condensation and bending of FtsZ filaments are important for the formation and constriction of the cytokinetic ring. PC190723 is an effective bactericidal cell division inhibitor that targets FtsZ in the pathogen *Staphylococcus aureus* and *Bacillus subtilis* and does not affect *Escherichia coli* cells, which apparently binds to a zone equivalent to the binding site of the anti-tumor drug taxol in tubulin (Haydon, D. J., Stokes, N. R., Ure, R., Galbraith, G., Bennett, J. M., Brown, D. R., Baker, P. J., Barynin, V. V., Rice, D. W., Sedelnikova, S. E., Heal, J. R., Sheridan, J. M., Aiwale, S. T., Chauhan, P. K., Srivastava, A., Taneja, A., Collins, I., Errington, J., and Czaplowski, L. G. (2008) *Science* 312, 1673–1675). We have found that the benzamide derivative PC190723 is an FtsZ polymer-stabilizing agent. PC190723 induced nucleated assembly of Bs-FtsZ into single-stranded coiled protofilaments and polymorphic condensates, including bundles, coils, and toroids, whose formation could be modulated with different solution conditions. Under conditions for reversible assembly of Bs-FtsZ, PC190723 binding reduced the GTPase activity and induced the formation of straight bundles and ribbons, which was also observed with Sa-FtsZ but not with nonsusceptible Ec-FtsZ. The fragment 2,6-difluoro-3-methoxybenzamide also induced Bs-FtsZ bundling. We propose that polymer stabilization by PC190723 suppresses *in vivo* FtsZ polymer dynamics and bacterial division. The biochemical action of PC190723 on FtsZ parallels that of the microtubule-stabilizing agent taxol on the eukaryotic structural homologue tubulin. Both taxol and PC190723 stabilize polymers against disassembly by preferential binding to each assembled protein. It is yet to be investigated whether both ligands target structurally related assembly switches.

^{*} This work was supported by Grants Ministerio de Ciencia (MCINN) BFU2008-00013 (to J. M. A.), Comunidad Autónoma de Madrid S-BIO-0214-2006 (to J. M. A. and O. L.), MCINN SAF2007-67008 (to M. L. L.-R.), S-SAL-249-2006 (to M. L. L.-R.), SAF2008-00451 (to O. L.), Red Temática de Investigación Cooperativa en Cáncer RD06-0020-1001 (to O. L.), Human Frontiers Science Program RGP39-2008 (to O. L.) and contracts Formación de Personal Investigación (to C. S.-B.), Consejo Superior de Investigaciones Científicas i3p (to S. H.), and Juan de la Cierva (to A. J. M.-G.).

^[5] The on-line version of this article (available at <http://www.jbc.org>) contains supplemental "Experimental Procedures," Table S1, and Figs. S1–S6.

[†] To whom correspondence should be addressed. Tel.: 34-918373112 (ext. 4381); Fax: 34-915360432; E-mail: j.m.andreu@cib.csic.es.

² Present address: Instituto de Estructura de la Materia, CSIC, Serrano 113 bis, 28006 Madrid, Spain.

Essential cell division protein FtsZ assembles into filaments that form the cytokinetic ring at the division site (1) and recruits the accessory proteins of the bacterial divisome (2–4). FtsZ, with an added membrane anchor, can form constricting rings in liposomes (5). FtsZ is a member of the tubulin family of cytoskeletal GTPases, also including $\alpha\beta$ -tubulin, γ -tubulin, bacterial tubulin BtubA/B (3, 6), and divergent TubZs (7). FtsZ and tubulin use the same structural fold and similar head-to-tail protofilaments with GTP bound at the intersubunit association interface (8), yet they have evolved to form different assemblies with specialized functions. Their GTPase sites are completed upon contact of the apical GTP-binding domain of one subunit with the basal GTPase activation domain of the next subunit. GTP hydrolysis renders the polymers metastable and ready for disassembly. There is evidence that unassembled tubulin, unlike other GTPases, is predominantly in an inactive (curved) conformation regardless of which nucleotide is bound and switches into the active (straight) conformation mainly through the assembly contacts and that GTP binding lowers the free energy barrier between both conformations (6, 9–11). Binding of the successful anti-tumor drug taxol overrides the GTP/GDP regulation, inducing microtubule assembly even with GDP (12, 13). Tubulin promiscuously interacts with small molecules of natural origin that induce or inhibit its assembly. However, there are fewer functional inhibitors for FtsZ.

FtsZ is a relatively simple assembly machine capable of nucleated linear polymerization. Such cooperative behavior of a linear polymer was anticipated by the self-switching assembly concept (14) and suggested to be possible for FtsZ if dimerization caused a conformational change that increases the affinity of the next monomer to bind (3, 15). Cryoelectron microscopy of unsupported samples has shown that FtsZ from *Escherichia coli* can form semiflexible single-stranded filaments (16). Their cooperative behavior is explained by an unfavorable monomer isomerization (activation switch) between an inactive, assembly incompetent, and active conformation, which is coupled to assembly, creating a nucleation barrier (16–19). On the other hand, FtsZ from *Methanococcus jannaschii* forms characteristic double-stranded filaments (20, 21). A number of crystal structures of FtsZ did not reveal a nucleotide-induced activation switch (22). The structural flexibility changes coupled to assembly are unknown, requiring determination of an FtsZ filament structure.

A cryoelectron tomography study of the *Caulobacter crescentus* cytoskeleton revealed a putative FtsZ ring, consisting of

FtsZ Assembly Induced by Small Antibacterial Molecule

a few short (100 nm) apparently single-stranded FtsZ filaments (5-nm wide) below the plasma membrane near the division site, and suggested that these FtsZ polymers generate the force that constricts the membrane for division through iterative cycles of GTP hydrolysis, depolymerization, and repolymerization (23). Lateral FtsZ filament association is also important for Z-ring formation and constriction. Several proteins are known to bundle FtsZ filaments, including ZipA, ZapA, and SepF (4). Helical FtsZ structures remodel by lateral association into the Z-ring in *Bacillus subtilis* (24), and artificial FtsZ rings coalesce into brighter rings (5). Several theoretical models for the Z-ring have proposed different roles for FtsZ filament condensation and bending (reviewed in Ref. 25).

FtsZ filaments are dynamic, with a subunit half-life of ~ 10 s, depending on the GTPase rate (26). Although FtsZ polymers can exchange nucleotides, GDP dissociation may be slow enough for polymer disassembly to take place first, resulting in the subunits of FtsZ polymers recycling with GTP hydrolysis (27, 28). The length dynamics of the small individual FtsZ filaments have not been determined.

Impairing FtsZ filament dynamics should block bacterial division. FtsZ has been recognized as an attractive target for new antibiotics (29) for emerging resistant pathogens. Expression of *ftsZ* is more stringently required for bacterial growth than the established antibacterial targets *murA* and *fabI* (30). Potentially druggable cavities in FtsZ structures (22) are the apical nucleotide-binding site and a lateral channel between the N- and C-terminal domains. The latter overlaps the binding site of the microtubule-stabilizing antitumor drug taxol in eukaryotic tubulin. Several GTP analogues substituted at C-8 selectively inhibit FtsZ polymerization but support tubulin assembly into microtubules (31), indicating differences in nucleotide binding by each protein that may be exploited to selectively inhibit bacterial FtsZ without poisoning eukaryotic tubulin. FtsZ recently has been validated as the target of an effective antibacterial compound developed as a cell division inhibitor in *B. subtilis* and the pathogen *Staphylococcus aureus*, PC190723. Its putative binding site, mapped with resistance mutations, corresponds to the taxol-binding site in tubulin (32).

We aimed to determine the mechanism of functional inhibition of FtsZ by the small antibacterial molecule PC190723, 3-[(6-chloro[1,3]thiazolo[5,4-*b*]pyridin-2-yl)methoxy]-2,6-difluorobenzamide (abbreviated here as PC).³ We have found that PC enhances the cooperative assembly of Bs-FtsZ into filaments, bundles, and other condensates. PC also is a Sa-FtsZ polymer stabilizer. Stabilizing FtsZ polymers should reduce their dynamics, which explains why PC blocks cell division in bacteria analogously to the action of taxol on tubulin.

³ The abbreviations used are: PC, 3-[(6-chloro[1,3]thiazolo[5,4-*b*]pyridin-2-yl)methoxy]-2,6-difluorobenzamide; Mes, 4-morpholineethanesulfonic acid; DFMB, 2,6-difluoro-3-methoxybenzamide; CTPM, (6-chloro[1,3]thiazolo[5,4-*b*]pyridin-2-yl)methanol; Bs-FtsZ, FtsZ from *B. subtilis*; Sa-FtsZ, FtsZ from *S. aureus*; Ec-FtsZ, FtsZ from *Escherichia coli*; Cr, critical protein concentration for polymerization; HPLC, high pressure liquid chromatography; GMPCPP, guanosine-5'-[(2, β)-methylene]triphosphate.

EXPERIMENTAL PROCEDURES

Methods for Bs-FtsZ, Ec-FtsZ, Sa-FtsZ, and tubulin purification, monitoring assembly with light scattering, electron microscopy, polymer pelleting, binding measurements, GTPase, and a screen of solution conditions for assembly are described under the supplemental "Experimental Procedures." PC190723 was provided by Prolysis (32). Stock solutions (1 mM) in deuterated dimethyl sulfoxide (Merck Uvasol) were kept frozen and dry. They were diluted directly into the experimental samples. Residual dimethyl sulfoxide was 2% (v/v) unless indicated. DFMB, 2,6-difluoro-3-hydroxybenzamide, and CTPM were synthesized in this work (supplemental data). Buffers employed were as follows: Hepes50 (50 mM Hepes/KOH, 50 mM KCl, 1 mM EDTA, pH 6.8), Hepes250 (50 mM Hepes/KOH, 250 mM KCl, 1 mM EDTA, pH 6.8) (where indicated, these buffers were made at pH 7.5), and Mes50 (50 mM Mes/KOH, 50 mM KCl, 1 mM EDTA, pH 6.5).

RESULTS

PC190723 induced Bs-FtsZ assembly into bundles and isolated filaments. These processes could be dissected and analyzed, employing different solution conditions, as described below.

PC Induces Bundles of *B. subtilis* FtsZ Filaments—To characterize the effects of PC on FtsZ assembly, full-length, untagged FtsZ from *B. subtilis* was first expressed and purified, and its reversible assembly was induced by 10 mM MgCl₂ and 2 mM GTP in Hepes50, 25 °C (see "Experimental Procedures") without other additives, which were chosen for convenience as reference conditions. Addition of PC induced a dramatic increase in FtsZ light scattering and stabilized polymers against disassembly induced by GDP (Fig. 1A). Many large PC-induced bundles and ribbons, in addition to FtsZ filaments, were observed by negative stain electron microscopy (Fig. 1B). These bundles and ribbons were several microns long, had a variable ~ 30 to ~ 60 nm width, and were apparently made of associated FtsZ filaments. Computed diffraction patterns indicated an axial spacing of 4.5 ± 0.5 nm between subunits (Fig. 1, C and D), which is compatible with the 4.3-nm spacing of FtsZ monomers associated head-to-tail in tubulin-like protofilaments (20, 21), and a shorter lateral spacing of 3.8 ± 0.3 nm, suggesting a lateral association of Bs-FtsZ molecules (Protein Data Bank code 2VXY; 32) in contact along their shortest dimension (that is, rotated $\sim 90^\circ$ on the longitudinal axis with respect to tubulin protofilaments in a microtubule) (33). PC-induced bundles and ribbons also formed with the slowly hydrolyzable GTP analogue GMPCPP (0.1 mM). Most FtsZ above a small ~ 0.3 μ M critical concentration (Cr) pelleted upon 20 min of centrifugation at $386,000 \times g$ (Fig. 1E). In the absence of PC, relatively short, ~ 4 -nm wide filaments were observed (Fig. 1F), which sedimented above a larger Cr ~ 5 μ M FtsZ. These results indicated that the small molecule PC stabilized Bs-FtsZ filament bundles but did not distinguish whether PC primarily enhances filament formation or bundling.

Effects of Solution Conditions, Mg²⁺ and Nucleotide—To elucidate the mechanism of PC-induced assembly and to characterize the effects of PC under more physiological conditions,

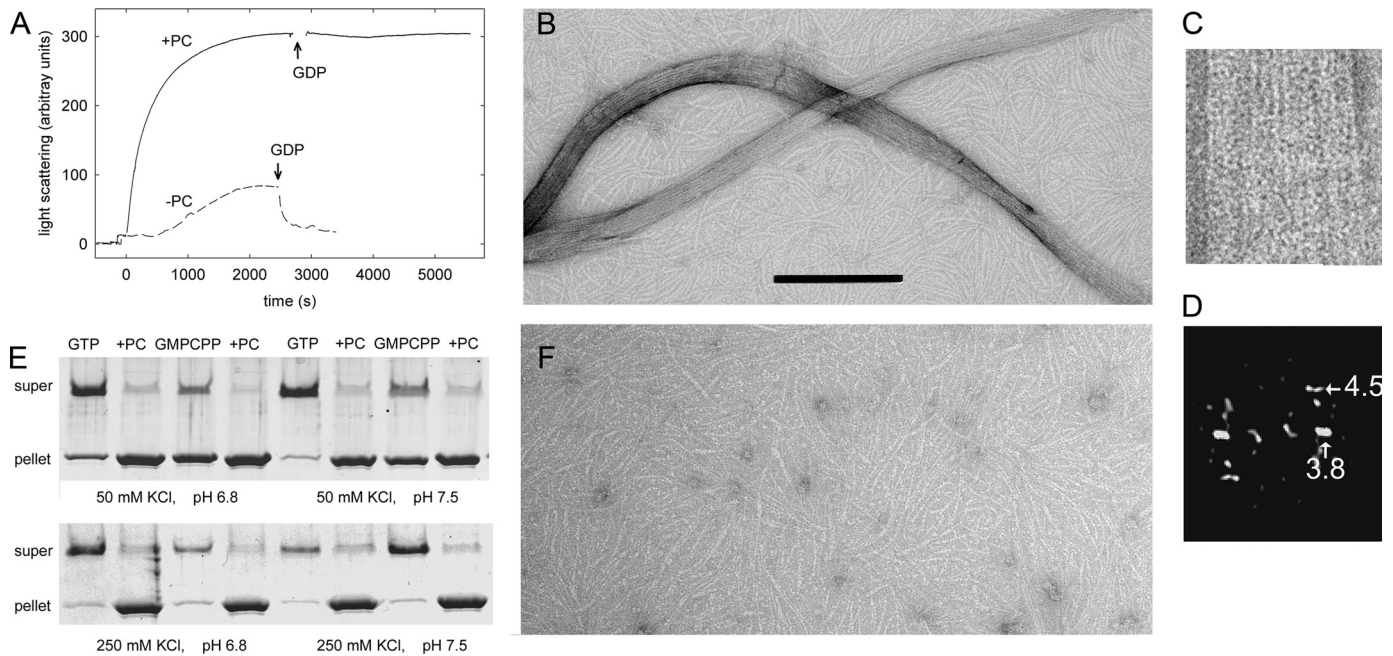


FIGURE 1. Assembly of bundles of Bs-FtsZ (10 μM) induced by PC (20 μM). A, light scattering time courses with and without PC in Hepes50 assembly buffer, 10 mM MgCl_2 , pH 6.8, 25 $^\circ\text{C}$. GTP (2 mM) was added at time 0 and 2 mM GDP as indicated by the arrows. B, electron micrograph of Bs-FtsZ with PC. Bar, 200 nm. C, an enlarged bundle. D, its computed diffractogram. The corresponding spacing of the main equatorial spot and the first layer line are indicated in nm. E, Bs-FtsZ polymer pelleting assays at varying pH and ionic strength. F, Bs-FtsZ without PC, magnified as in B.

pH was increased to 7.5, or ionic strength increased to 250 mM KCl, which reduced the extent of spontaneous Bs-FtsZ assembly with nucleotide and Mg^{2+} . Assembly was efficiently induced by PC in these cases (Fig. 1E), although bundle formation was reduced. Assembly was markedly sensitive to the buffer anion (supplemental “Experimental Procedures”). Disassembly could be monitored by light scattering following assembly of 10 μM Bs-FtsZ with 25 μM GMPCPP (expected to stabilize polymers) and 10 mM MgCl_2 in 250 mM KCl (scattering with GTP was very small). This was attributed to GMPCPP hydrolysis and was not observed in the presence of PC. GTP or GMPCPP was required for PC-enhanced assembly. Mg^{2+} without nucleotide was ineffective. Interestingly, GTP or GMPCPP without Mg^{2+} induced assembly of Bs-FtsZ filaments, which were not formed with GDP or GMPCP. Mg^{2+} plus GDP or GMPCP and PC gave a weak polymer formation. These results confirmed that PC stabilizes Bs-FtsZ polymers and showed the requirement of the nucleotide γ -phosphate.

It was possible to separate PC-induced filament assembly from bundle formation by using 250 mM KCl and GMPCPP. Bs-FtsZ assembly was only incipient without Mg^{2+} (Fig. 2A). Adding only PC induced characteristic filament coils (Fig. 2B), whereas Mg^{2+} alone induced the formation of filaments (Fig. 2C). Both were inhibited with GMPCP. PC and Mg^{2+} together induced the formation of filaments and bundles (Fig. 2D). Similar results were obtained with GTP, but with PC and Mg^{2+} , dense coils and no bundles were observed (supplemental Fig. S1).

PC Induces Bs-FtsZ Single-stranded Filament Assembly— Mg^{2+} -less Hepes250 buffer permitted PC-induced nucleated assembly of single-stranded Bs-FtsZ filaments. Our divalent cation-free solutions typically contain $\sim 1 \mu\text{M}$ residual Mg^{2+} (34) that with 1 mM EDTA in buffer results in $\sim 4 \text{ nM}$ free Mg^{2+} .

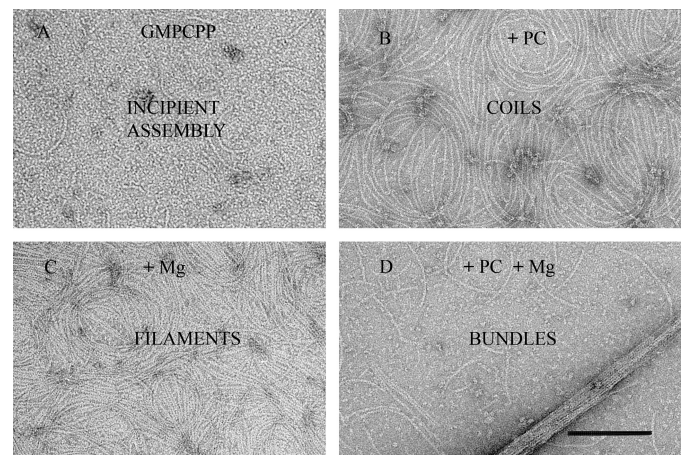


FIGURE 2. PC and magnesium-induced Bs-FtsZ assemblies. Electron micrograph of negatively stained polymers formed by Bs-FtsZ (10 μM) in Hepes250 assembly buffer with 0.1 mM GMPCPP (A), 0.1 mM GMPCPP and 20 μM PC (B), 0.1 mM GMPCPP and 10 mM MgCl_2 (C), and 0.1 mM GMPCPP and 10 mM MgCl_2 and 20 μM PC (D). The bar indicates 200 nm.

Incipient assembly of Bs-FtsZ was observed with nucleotide in the absence of PC (no nucleotide-induced light scattering increase or pelleting). However, addition of PC under these conditions resulted in Bs-FtsZ polymerization. There was a small light scattering increase with PC and GMPCPP (Fig. 3A). These PC-induced FtsZ filaments sedimented in 80 min at $386,000 \times g$, which allowed their quantification. Practically all Bs-FtsZ was pelleted with PC and GTP or GMPCPP above a $\text{Cr} \sim 1 \mu\text{M}$ (Fig. 3B; GTP, $0.8 \pm 0.1 \mu\text{M}$; GMPCPP, $1.3 \pm 0.3 \mu\text{M}$). Insignificant GTP hydrolysis was detected under these conditions. These results indicated a nucleated polymerization mechanism for the PC-induced assembly of Bs-FtsZ filaments, with an apparent free energy change for polymer elongation

FtsZ Assembly Induced by Small Antibacterial Molecule

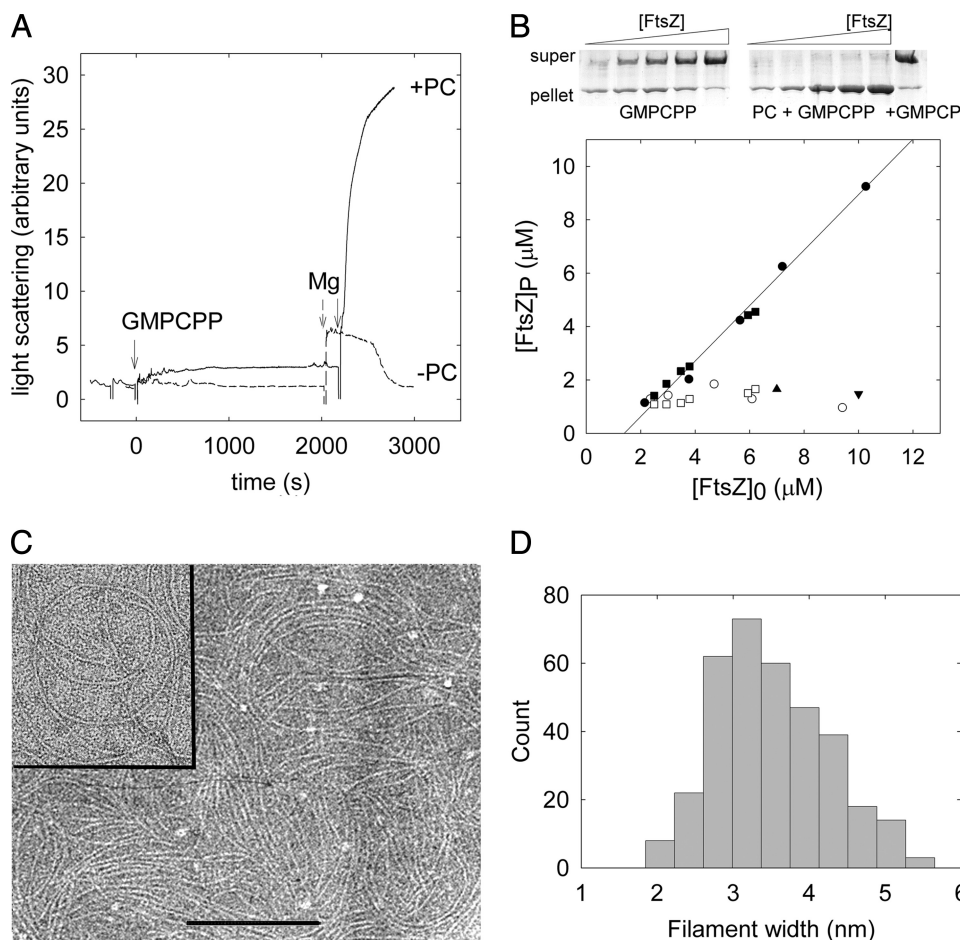


FIGURE 3. Bs-FtsZ filament assembly induced by PC. *A*, solid line, light scattering changes induced on Bs-FtsZ (10 μM) with PC (20 μM) by additions of GMPCPP (25 μM) and MgCl_2 (10 mM) (arrows) in Hepes250, pH 6.8, 25 $^\circ\text{C}$. Dashed line, same without PC. *B*, example of sedimentation of Bs-FtsZ polymers formed without Mg^{2+} (top) and pellet quantification (bottom). Filled circles, PC and GMPCPP (0.1 mM); filled squares, PC and GTP (2 mM); open symbols, without PC; triangle, PC and GDP; inverted triangle, PC and GMPCPP. *C*, cryoelectron micrograph of Bs-FtsZ filaments assembled with PC and GTP under the same conditions without Mg^{2+} . Inset, negatively stained filaments. Bar, 200 nm. *D*, cryoelectron microscopy filament width distribution, indicating that the filaments are one Bs-FtsZ molecule-wide.

$\Delta G_{\text{app}}^0 = RT \ln Cr = -8.2 \text{ kcal mol}^{-1}$ (16). With GTP or GMPCPP and no PC, a background similar to that of PC and GDP or GMPCP was observed (Fig. 3*B*). Cr decreased to insignificant values in experiments made in parallel with 10 mM MgCl_2 (supplemental Fig. S2), indicating a larger effective elongation affinity, although the system was not at chemical equilibrium due to nucleotide hydrolysis. Interestingly, the PC-induced Bs-FtsZ filaments without Mg^{2+} typically had an $\sim 100\text{-nm}$ curvature radius and appeared single-stranded. To confirm that these filaments are single-stranded, we performed cryoelectron microscopy under these conditions, using holey carbon film. The sample trapped within the small holes was quickly vitrified and kept under liquid nitrogen temperatures to rule out any effect of the staining agent or the adsorption to a support film (Fig. 3*C*). Filament width measurements from the cryomicrographs had a distribution with an average $3.5 \pm 0.7 \text{ nm}$ (Fig. 3*D*), indicating that these filaments are one Bs-FtsZ molecule wide.

Binding of PC and Its Fragment DFMB to Bs-FtsZ Polymers— Titrations of Bs-FtsZ polymer formation with PC showed an increasing fraction of sedimented FtsZ, which saturated

between 0.5 and 1 PC per FtsZ (Fig. 4*A*), compatible with PC inducing polymerization by binding to one site in FtsZ. For a ligand to induce protein association, it has to bind more to the protein polymer than the monomer. As a first approach, PC binding to Bs-FtsZ polymers was determined by extraction of the ligand from the pellets and supernatants followed by HPLC. PC cosedimented with the polymers and inhibition of polymerization with GDP also inhibited the PC pull-down. The results were 0.5 PC bound per FtsZ at $\sim 10 \mu\text{M}$ free PC, irrespective of ionic strength and magnesium level (0.46 ± 0.14 in Hepes50 with 10 mM MgCl_2 , 0.40 ± 0.10 in Hepes250 without MgCl_2 , and 0.54 ± 0.10 in Hepes250 with 10 mM MgCl_2). FtsZ was active in polymer formation (Fig. 3*B*), and saturating the binding to an expected 1 PC per FtsZ was precluded by the free ligand solubility ($\sim 10 \mu\text{M}$ in our buffers). The simplest interpretation of these results is one PC binding site per polymer FtsZ molecule with an apparent affinity $\sim 10^5 \text{ M}^{-1}$.

Interestingly, the PC fragment DFMB (1–4 mM; Fig. 5, *A* and *C*), 2,6-difluoro-3-hydroxybenzamide (1–4 mM) and to a lesser extent 3-methoxybenzamide (20 mM), were found to induce large Bs-FtsZ bundles similar to those obtained

with PC (20 μM), thus following their relative antibacterial activities (35). The other fragment of the PC molecule, CTPM (1 mM) did not induce Bs-FtsZ bundling (Fig. 5, *B* and *C*). These results suggested specific but weak binding of DFMB to Bs-FtsZ polymers, which could not be accurately measured by pelleting HPLC. DFMB has an $\sim 10^2$ -fold higher effective concentration than PC, suggesting a two order of magnitude lower affinity. Note that if PC were a nonself-associating ideal bifunctional ligand (36), the rest of the molecule, if isolated, would be expected to bind more weakly than DFMB and be inactive below $\sim 0.5 \text{ M}$.

Modulation of the GTPase Activity of Bs-FtsZ by PC— The effects of PC on the GTPase activity of polymerizing Bs-FtsZ solutions was examined with 10 mM MgCl_2 in three buffers that give quite different degrees of PC-induced bundling (see above). Control GTPase without PC was dependent on the KCl concentration: $0.61 \pm 0.09 \text{ min}^{-1}$ in Hepes250, $0.22 \pm 0.02 \text{ min}^{-1}$ in Hepes50, $0.15 \pm 0.08 \text{ min}^{-1}$ in Mes50. A partial inhibition of the GTPase rate was observed with PC, to a similar extent (Fig. 6) irrespective of the buffer. The inhibition between ~ 1 and $\sim 10 \mu\text{M}$ PC roughly paralleled the formation of pellet-

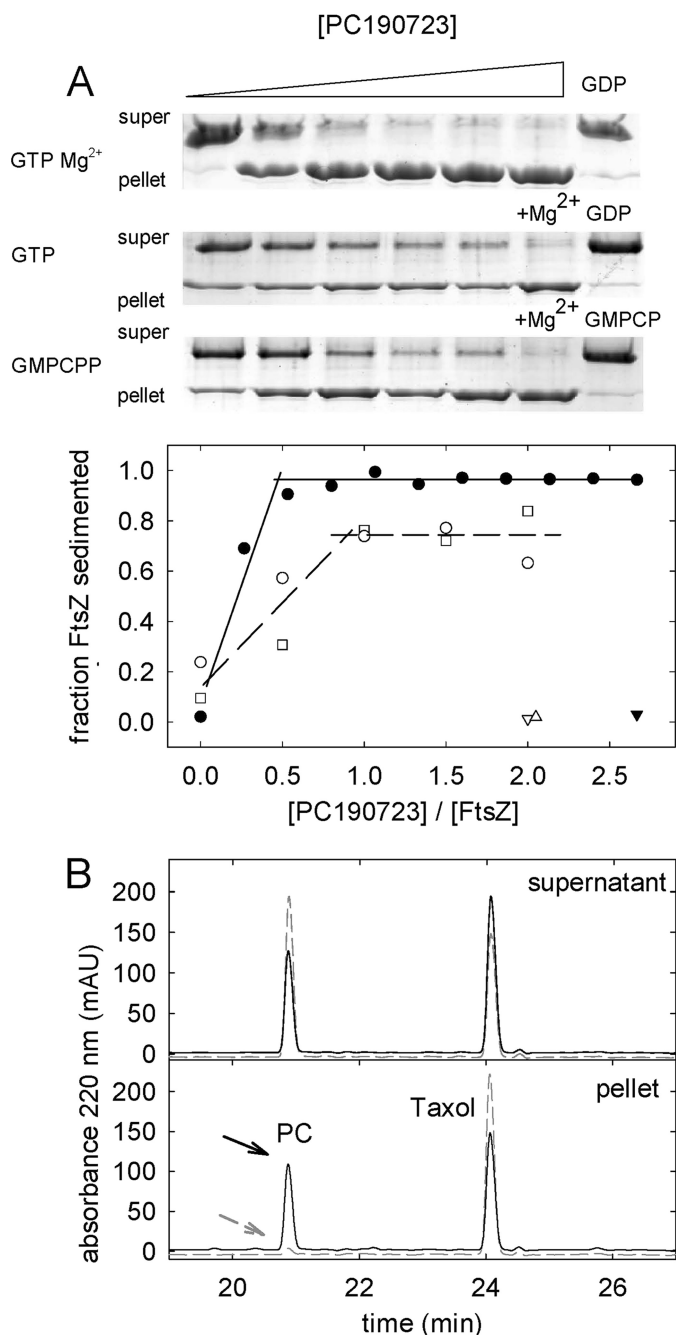


FIGURE 4. Binding of PC to Bs-FtsZ polymers. *A*, Bs-FtsZ (10 μ M) sedimentation assays in Hepes250, pH 6.8, 25 $^{\circ}$ C, and quantification of polymer with increasing concentrations of PC. *Open circles*, with 2 mM GTP; *filled circles*, with 2 mM GTP and Mg²⁺; *void squares*, with 0.1 mM GMPCPP. *Triangles*, corresponding data with GDP, GDP, and Mg²⁺ or GMPCPP. *B*, HPLC analysis of PC (10 μ M total) co-sedimentation with Bs-FtsZ polymers. *Solid lines and arrow*, with GTP and Mg²⁺; *dashed gray lines and arrow*, control with GDP and Mg²⁺. Taxol is an internal standard here. In this experiment, the pelleted PC and FtsZ were 4.8 and 10 μ M, respectively. *mAU*, milliabsorbance units.

able polymer (Fig. 4A). Low PC concentrations variably enhanced the relative GTPase activity in Hepes250. This may be a simple consequence of a large increase in FtsZ GTPase upon polymerization relative to the weakly polymerizing control without PC (Fig. 1E) (since the rate measured is per total FtsZ, not per assembled FtsZ). Control measurements showed that ³H[GTP] binding to Bs-FtsZ and to Ec-FtsZ was not modified by PC (supplemental Fig. S3).

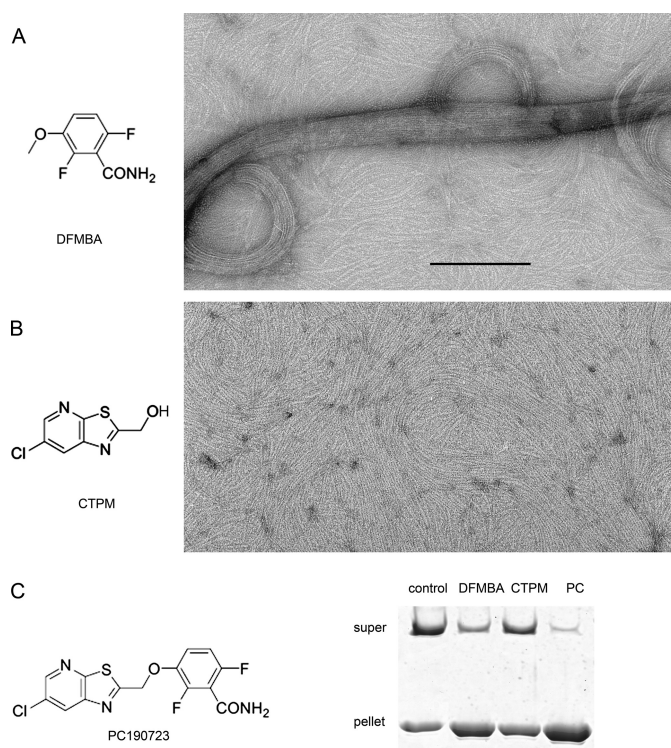


FIGURE 5. Bs-FtsZ polymers induced by PC fragments in Mes50 assembly buffer with 10 mM MgCl₂ and 2 mM GTP. *A*, 1 mM fragment of DFMBAs. *B*, 1 mM fragment of analogue CTPM (similar to control without fragment, as in Fig. 1F). *Bar*, 200 nm. *C*, chemical structure of PC and low speed FtsZ polymers pelleting (15,000 \times *g*, 20 min) under the same conditions (PC, 20 μ M). DFMBAs also induced a FtsZ light scattering increase that was not observed with CTPM. The Cr for assembly in Hepes50 was reduced from \sim 5 μ M to \sim 1 μ M FtsZ with DFMBAs (4 mM).

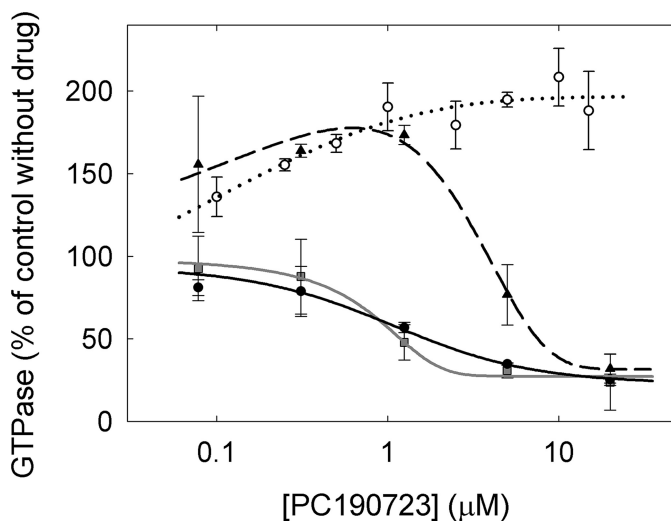


FIGURE 6. Effects of PC on the GTPase activity of FtsZ (10 μ M), with 1 mM GTP and 10 mM MgCl₂, pH 6.8 at 25 $^{\circ}$ C. Bs-FtsZ: *solid circles*, Hepes50; *triangles*, Hepes250; *squares*, Mes50. Ec-FtsZ: *open circles*, Hepes50 (average of three different protein preparations). The *lines* are drawn solely to show the trend of the data. The increase in GTPase activity of Ec-FtsZ was confirmed by measurements at varying protein concentrations with excess 15 μ M PC (not shown).

Formation of Polymorphic Bs-FtsZ Filament Condensates with Different Curvatures—Bs-FtsZ filaments frequently adopted bow shapes and easily coalesced into coils or associ-

FtsZ Assembly Induced by Small Antibacterial Molecule

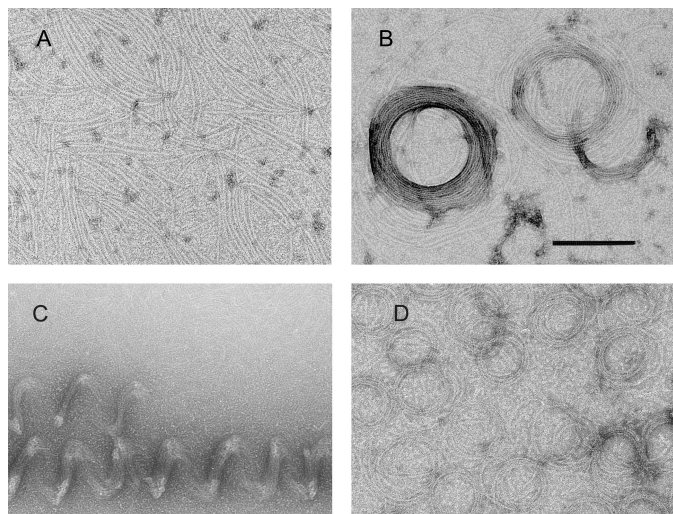


FIGURE 7. Polymorphic assemblies of Bs-FtsZ, in addition to bundles and ribbons (see Fig. 1B). A, filaments observed in Hepes50, pH 6.8, with GTP and PC. B, toroids in another field of the same sample. C, helical bundles in Hepes50 at pH 7.5 with GTP, 10 mM MgCl₂, and PC. D, coiled filaments and toroids formed without PC or dimethyl sulfoxide in Mes50 with MgCl₂ and GMPCPP. Similar polymers were observed in Hepes50, pH 6.8, or with GTP. Bar, 200 nm.

ated into straight bundles (see above). Other Bs-FtsZ filament condensates also observed include toroids and helical bundles (see supplemental Table S1 for a list of polymorphs and conditions). Briefly, along with filaments formed with GTP and PC (Fig. 7A) and filament coils (similar to Fig. 2B), toroids ~300 nm in diameter were observed on the same grids (Fig. 7B). Large helical bundles were observed at pH 7.5 with PC, GTP, and Mg²⁺ (Fig. 7C). Interestingly, Bs-FtsZ condensates could also form in the absence of PC with GMPCPP and Mg²⁺ as coils, and smaller toroids ~150 nm in diameter were observed (Fig. 7D).

Specificity of FtsZ-PC Interactions—We next compared the effects of PC on the assembly of FtsZ from susceptible (*B. subtilis* and *S. aureus*) and nonsusceptible (*E. coli*) bacteria in Hepes50 (Fig. 8A). The weak formation of pelletable polymer by Sa-FtsZ was markedly enhanced by PC, at concentrations higher than with Bs-FtsZ. A large PC-induced increase in Sa-FtsZ light scattering was observed with nucleotide and Mg²⁺ (supplemental Fig. S4). Electron micrographs showed a transformation of Sa-FtsZ oligomers (Fig. 8B) into coils, toroids, and straight bundles with PC (Fig. 8, C and D). DFMBAs had similar effects at higher concentrations. On the other hand, PC induced bundling was not observed with Ec-FtsZ. Filament morphology was not modified (Fig. 8E), and changes in polymerization were insignificant when employing a GTP-regenerating system (Fig. 8A). Unexpectedly, PC induced a faster disassembly without a GTP regenerating system (supplemental Fig. S4C) and a 2-fold enhancement of Ec-FtsZ GTPase (Fig. 6). HPLC measurements (with 10 μM Ec-FtsZ and 20 μM PC) indicated binding of 0.4 PC per polymerized Ec-FtsZ, although it did not induce bundling. Finally, PC (20 μM) or DFMBAs (4 mM) did not affect the assembly of the more distant eukaryotic homologue αβ-tubulin (15 μM) in light scattering tests, or the gross morphology (in electron microscopy) of the microtubular polymers formed (not shown).

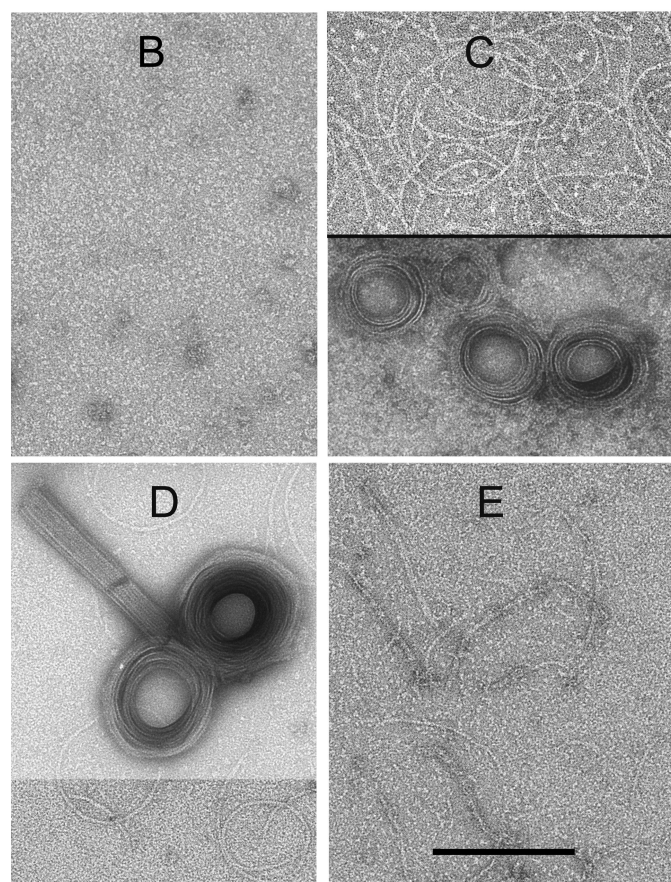
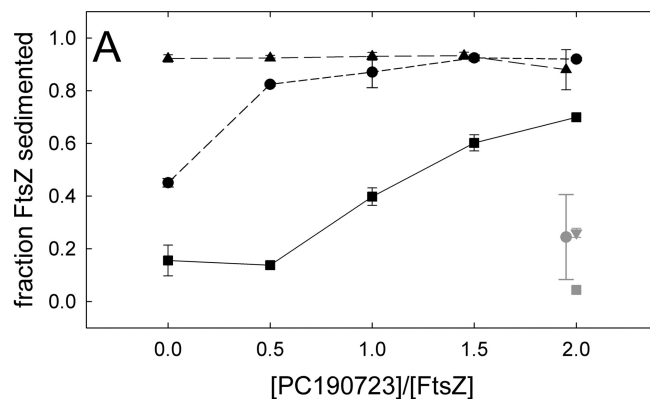


FIGURE 8. Effects of PC on the polymerization of FtsZ (10 μM) from susceptible (*B. subtilis* and *S. aureus*) and resistant (*E. coli*) bacteria. A, FtsZ polymer versus PC concentration. Circles, Bs-FtsZ; squares, Sa-FtsZ; triangles, Ec-FtsZ. The gray symbols are corresponding controls without magnesium. The conditions were Hepes50 buffer with 10 mM MgCl₂ and 1 mM GTP, pH 6.8, 25 °C. A GTP regenerating system (1 unit/ml acetate kinase and 15 mM acetyl phosphate) was added for the measurements in A. This was required to reproducibly pellet the Ec-FtsZ polymers in the experiment time and did not modify the pelleting of Bs-FtsZ and Sa-FtsZ. B–D, electron micrographs of Sa-FtsZ with GTP (B), with GTP and 20 μM PC in two fields from the same sample (C) and with 0.1 mM GMPCPP and 20 μM PC (D, upper panel displayed with reduced contrast). E, Ec-FtsZ filaments with GTP and 20 μM PC. Controls without PC gave similar images. Bar, 200 nm.

DISCUSSION

We have shown in this study that binding of the small antibacterial molecule PC190723 enhances the assembly of purified cell division protein Bs-FtsZ into filaments and bundles. Preventing disassembly of FtsZ polymers should inhibit their func-

tional dynamics *in vivo*, which we propose explains cytokinesis inhibition. This is supported by the observation of FtsZ foci along PC-treated bacilli instead of Z-rings (32).

Our results also give insight into the mechanisms of FtsZ assembly and facilitate the use of PC as a tool to investigate the biological role of FtsZ. PC binding induces Bs-FtsZ filament formation under incipient assembly conditions (250 mM KCl, no Mg^{2+}). These filaments are single stranded, yet they assemble with a cooperative critical concentration behavior, typical of multi-stranded polymers. This may be explained by Bs-FtsZ switching between inactive and active states similarly to Ec-FtsZ (16), indicating that PC induces the polymer Bs-FtsZ conformation, possibly by drugging its assembly switch. However, it cannot be ruled out that the cooperative behavior of Bs-FtsZ with PC might be caused by some filament cyclization in the coils observed or by filament network formation. Direct measurements of PC binding to FtsZ polymers suggest partial saturation of one PC binding site in FtsZ, limited by the solubility of the ligand. PC-induced Bs-FtsZ filament assembly in the absence of magnesium proceeds without GTP hydrolysis, constituting an equilibrium model system of ligand-induced nucleated assembly, analogous to the taxol-induced assembly of GDP-tubulin (12). It would be worth studying in more detail the linkage of PC binding to FtsZ filament assembly.

The FtsZ GTPase site is at the axial interface between consecutive FtsZ molecules in a protofilament (8, 37), so that GTP hydrolysis takes place upon FtsZ assembly. PC modulates the GTPase activity of steady-state polymerizing Bs-FtsZ solutions. The GTPase activation at early stages of assembly remains to be studied. Focusing on the effects of the higher PC concentrations, the partial inhibition of Bs-FtsZ GTPase and the lack of PC effect of GTP binding argue against binding to the same site. This GTPase inhibition is difficult to explain by a bundling effect, due to the coincident extent of inhibition under different bundling conditions (Fig. 6). Mechanistically, PC binding at a site different from the GTP site may either decrease the FtsZ subunit turnover in stabilized filaments and therefore the GTP hydrolysis turnover (27) or allosterically modulate (32) the GTP hydrolysis and exchange in FtsZ filaments.

Depending on the solution conditions, the assembly of Bs-FtsZ varies and so does the effect of PC, with a similar global assembly enhancement. PC binding under Bs-FtsZ filament assembly conditions (50 mM KCl, Mg^{2+}) results in the formation of large condensates of Bs-FtsZ filaments. This may be a consequence of filament accumulation, or PC might induce the condensation of existing filaments, by binding more to condensed than to isolated FtsZ filaments. PC induces, in addition to characteristically curved Bs-FtsZ filaments and straight bundles (Fig. 1), toroids at pH 6.8 and helical bundles at pH 7.5 (Fig. 7), underscoring the flexibility of FtsZ filaments. The observation of Bs-FtsZ coils and toroids formed with nucleotide and Mg^{2+} in the absence of PC (Fig. 7) indicate that the ability to form curved condensates is an intrinsic property of Bs-FtsZ filaments, which is important for the formation of the Z-ring (24), and is enhanced by PC binding. Curved FtsZ filaments coalescing into the Z-ring have recently been proposed to generate the constriction force (38).

We have employed Bs-FtsZ as a model and confirmed that PC also induces bundling of Sa-FtsZ, but does not induce assembly or condensation of Ec-FtsZ filaments. This is in agreement with the antibacterial spectrum of PC, which has been related to the presence of Val307 in FtsZ from susceptible organisms (32). Mutations conferring resistance to PC cluster at the long channel between the two domains of the FtsZ molecule where PC has been docked (32). This zone is different from the GTP binding site and it overlaps the taxol binding site in β -tubulin. In agreement with the large sequence divergence between both proteins no marked cross reactions have been observed (32; Results). In order to stabilize susceptible FtsZ polymers PC should bind more to them than to monomers. It could be thought that PC does not bind to FtsZ monomers, nor fits well into the binding site of non-susceptible FtsZ (32). However, the GTPase enhancement and HPLC measurements indicate PC binding to Ec-FtsZ. Given that PC did not modify steady-state polymerization, it should bind similarly to the monomers and polymers of this non-susceptible FtsZ. This binding could occur in a different manner (ineffectively or at another site) than in susceptible Bs-FtsZ and Sa-FtsZ polymers. The as yet unresolved atomic structure of an FtsZ-PC complex could give insight into the detailed structural mechanism of PC action, possibly the FtsZ activation switch, and would facilitate the optimization of PC-derived drugs targeting FtsZ in bacterial pathogens. The major determinant of PC binding to FtsZ (Results) and antibacterial activity (35) appears to be its DFMBBA moiety.

An increasing number of proteins are known to modulate FtsZ assembly (4), inhibiting or enhancing FtsZ polymerization and bundling. Small molecules reported to stabilize FtsZ polymers include zantrins 3 and 5 (39), ruthenium red (40) and DAPI (41), and very recently FtsZ bundling by the benzoic acid derivative OTBA (42) has been proposed as a strategy to inhibit bacterial division. It would be of interest to know whether these molecules share the PC site or bind elsewhere in FtsZ. It is known that Ca^{2+} ions induce FtsZ filament bundling (43, 44) and that FtsZ condensates can form in a nonspecific manner by macromolecular crowding (45) or by interactions with polar molecules at relatively high concentrations (46). Volume exclusion in the bacterial cytosol should favor the formation of FtsZ condensates. An important question is whether there are endogenous regulators sharing the PC binding site of FtsZ.

The biochemical action of PC on FtsZ polymers parallels that of taxol on tubulin (12), since each drug stabilizes its respective protein polymers against disassembly, by binding more to polymers than to monomers. Taxol was the first (47) among antitumor Microtubule Stabilizing Agents, which impair cellular microtubule dynamics and mitosis, triggering cell death (48). Microtubule Stabilizing Agents work by preferential binding to assembled tubulin (49). The structural mechanism coupling taxol binding and microtubule assembly is currently under investigation (50). In the case of the PC-induced FtsZ filaments the problem may be simpler due to the lack of lateral interactions. At a cellular level, multiple microtubule asters form in tumor cells treated with

high taxol concentrations, instead of normal spindles (Fig. S5; 51). Multiple mislocalized FtsZ foci, instead of a functional Z-ring, form along PC-treated bacteria, which appear to cause the inhibition of cytokinesis leading to bacterial lysis by PC (32). We speculate that PC is the first of a new class of synthetic antibacterials, the FtsZ Polymer Stabilizing Agents. Our findings raise the question of whether taxol and PC have totally different structural mechanisms of action or, by binding to equivalent sites, to what extent each of them acts on a conserved assembly switch in the tubulin-FtsZ superfamily of proteins.

Acknowledgments—We thank N. Stokes and Prolysis for PC190723, M. A. Oliva and J. Löwe for the Bs-FtsZ expression plasmid, J. Jimenez-Barbero for encouragement, P. Chacón and J. F. Díaz for discussions, and D. Juan for technical assistance.

REFERENCES

- Bi, E. F., and Lutkenhaus, J. (1991) *Nature* **354**, 161–164
- Margolin, W. (2005) *Nat. Rev. Mol. Cell Biol.* **6**, 862–871
- Michie, K. A., and Löwe, J. (2006) *Annu. Rev. Biochem.* **75**, 467–492
- Adams, D. W., and Errington, J. (2009) *Nat. Rev. Microbiol.* **7**, 642–653
- Osawa, M., Anderson, D. E., and Erickson, H. P. (2008) *Science* **320**, 792–794
- Buey, R. M., Díaz, J. F., and Andreu, J. M. (2006) *Biochemistry* **45**, 5933–5938
- Larsen, R. A., Cusumano, C., Fujioka, A., Lim-Fong, G., Patterson, P., and Pogliano, J. (2007) *Genes Dev.* **21**, 1340–1352
- Nogales, E., Downing, K. H., Amos, L. A., and Löwe, J. (1998) *Nat. Struct. Biol.* **5**, 451–458
- Rice, L. M., Montabana, E. A., and Agard, D. A. (2008) *Proc. Natl. Acad. Sci. U.S.A.* **105**, 5378–5383
- Gebremichael, Y., Chu, J. W., and Voth, G. A. (2008) *Biophys. J.* **95**, 2487–2499
- Bennett, M. J., Chik, J. K., Slys, G. W., Luchko, T., Tuszyński, J., Sackett, D. L., and Schriemer, D. C. (2009) *Biochemistry* **48**, 4858–4870
- Díaz, J. F., Menéndez, M., and Andreu, J. M. (1993) *Biochemistry* **32**, 10067–10077
- Elie-Caille, C., Severin, F., Helenius, J., Howard, J., Muller, D. J., and Hyman, A. A. (2007) *Curr. Biol.* **17**, 1765–1770
- Caspar, D.L. (1980) *Biophys. J.* **32**, 103–138
- Dajkovic, A., and Lutkenhaus, J. (2006) *J. Mol. Microbiol. Biotechnol.* **11**, 140–151
- Huecas, S., Llorca, O., Boskovic, J., Martín-Benito, J., Valpuesta, J. M., and Andreu, J. M. (2008) *Biophys. J.* **94**, 1796–1806
- Dajkovic, A., Mukherjee, A., and Lutkenhaus, J. (2008) *J. Bacteriol.* **190**, 2513–2526
- Miraldi, E. R., Thomas, P. J., and Romberg, L. (2008) *Biophys. J.* **95**, 2470–2486
- Lan, G., Dajkovic, A., Wirtz, D., and Sun, S. X. (2008) *Biophys. J.* **95**, 4045–4056
- Löwe, J., and Amos, L. A. (1999) *EMBO J.* **18**, 2364–2371
- Oliva, M. A., Huecas, S., Palacios, J. M., Martín-Benito, J., Valpuesta, J. M., and Andreu, J. M. (2003) *J. Biol. Chem.* **278**, 33562–33570
- Oliva, M. A., Trambaiolo, D., and Löwe, J. (2007) *J. Mol. Biol.* **373**, 1229–1242
- Li, Z., Trimble, M. J., Brun, Y. V., and Jensen, G. J. (2007) *EMBO J.* **26**, 4694–4708
- Monahan, L. G., Robinson, A., and Harry, E. J. (2009) *Mol. Microbiol.* **74**, 1004–1017
- Erickson, H. P. (2009) *Proc. Natl. Acad. Sci. U.S.A.* **106**, 9238–9243
- Stricker, J., Maddox, P., Salmon, E. D., and Erickson, H. P. (2002) *Proc. Natl. Acad. Sci. U.S.A.* **99**, 3171–3175
- Huecas, S., Schaffner-Barbero, C., García, W., Yébenes, H., Palacios, J. M., Díaz, J. F., Menéndez, M., and Andreu, J. M. (2007) *J. Biol. Chem.* **282**, 37515–37528
- Chen, Y., and Erickson, H. P. (2009) *Biochemistry* **48**, 6664–6673
- Vollmer, W. (2006) *Appl. Microbiol. Biotechnol.* **73**, 37–47
- Goh, S., Boberek, J. M., Nakashima, N., Stach, J., and Good, L. (2009) *PLoS One* **4**, e6061
- Läpchen, T., Pinas, V. A., Hartog, A. F., Koomen, G. J., Schaffner-Barbero, C., Andreu, J. M., Trambaiolo, D., Löwe, J., Juhem, A., Popov, A. V., and den Blaauwen, T. (2008) *Chem. Biol.* **15**, 189–199
- Haydon, D. J., Stokes, N. R., Ure, R., Galbraith, G., Bennett, J. M., Brown, D. R., Baker, P. J., Barynin, V. V., Rice, D. W., Sedelnikova, S. E., Heal, J. R., Sheridan, J. M., Aiwale, S. T., Chauhan, P. K., Srivastava, A., Taneja, A., Collins, I., Errington, J., and Czaplowski, L. G. (2008) *Science* **321**, 1673–1675
- Nogales, E., Whittaker, M., Milligan, R. A., and Downing, K. H. (1999) *Cell* **96**, 79–88
- Rivas, G., López, A., Mingorance, J., Ferrándiz, M. J., Zorrilla, S., Minton, A. P., Vicente, M., and Andreu, J. M. (2000) *J. Biol. Chem.* **275**, 11740–11749
- Czaplowski, L. G., Collins, I., Boyd, E. A., Brown, D., East, S. P., Gardiner, M., Fletcher, R., Haydon, D. J., Henstock, V., Ingram, P., Jones, C., Noula, C., Kennison, L., Rockley, C., Rose, V., Thomaidis-Brears, H. B., Ure, R., Whittaker, M., and Stokes, N. R. (2009) *Bioorg. Med. Chem. Lett.* **19**, 524–527
- Andreu, J. M., and Timasheff, S. N. (1982) *Biochemistry* **21**, 534–543
- Oliva, M. A., Cordell, S. C., and Löwe, J. (2004) *Nat. Struct. Mol. Biol.* **11**, 1243–1250
- Osawa, M., Anderson, D. E., and Erickson, H. P. (2009) *EMBO J.* **28**, 3476–3784
- Margalit, D. N., Romberg, L., Mets, R. B., Hebert, A. M., Mitchison, T. J., Kirschner, M. W., and RayChaudhuri, D. (2004) *Proc. Natl. Acad. Sci. U.S.A.* **101**, 11821–11826
- Santra, M. K., Beuria, T. K., Banerjee, A., and Panda, D. (2004) *J. Biol. Chem.* **279**, 25959–25965
- Nova, E., Montecinos, F., Brunet, J. E., Lagos, R., and Monasterio, O. (2007) *Arch. Biochem. Biophys.* **465**, 315–319
- Beuria, T. K., Singh, P., Surolia, A., and Panda, D. (2009) *Biochem. J.* **423**, 61–69
- Yu, X. C., and Margolin, W. (1997) *EMBO J.* **16**, 5455–5463
- Marrington, R., Small, E., Rodger, A., Dafforn, T. R., and Addinall, S. G. (2004) *J. Biol. Chem.* **279**, 48821–48829
- González, J. M., Jiménez, M., Vélez, M., Mingorance, J., Andreu, J. M., Vicente, M., and Rivas, G. (2003) *J. Biol. Chem.* **278**, 37664–37671
- Popp, D., Iwasa, M., Narita, A., Erickson, H. P., and Maéda, Y. (2009) *Biopolymers* **91**, 340–350
- Schiff, P. B., Fant, J., and Horwitz, S. B. (1979) *Nature* **277**, 665–667
- Jordan, M. A., and Wilson, L. (2004) *Nat. Rev. Cancer* **4**, 253–265
- Díaz, J. F., Andreu, J. M., and Jimenez-Barbero, J. (2009) *Topics Curr. Chem.* **286**, 121–149
- Xiao, H., Verdier-Pinard, P., Fernandez-Fuentes, N., Burd, B., Angeletti, R., Fiser, A., Horwitz, S. B., and Orr, G. A. (2006) *Proc. Natl. Acad. Sci. U.S.A.* **103**, 10166–10173
- Abal, M., Souto, A. A., Amat-Guerri, F., Acuña, A. U., Andreu, J. M., and Barasoain, I. (2001) *Cell Motil. Cytoskeleton* **49**, 1–15

Supplemental Data

EXPERIMENTAL PROCEDURES

Proteins expression and purification. Untagged, full-length *ftsZ* from *B. subtilis* (ATCC 23857D) cloned into pHis17 (1) was sequenced. The deduced protein sequence was identical to the Uniprot *B. subtilis* FtsZ sequence P17865 (16 June 2009). The construction was transformed into *E. coli* C41(DE3) cells, grown in 2xYT medium (1L) with 100ug/mL ampicillin and expression induced with 1 mM IPTG (at $Abs_{600nm} = 0.5$, 3h at 37 °C). The cell pellet was resuspended in 20 ml of TKM buffer (50 mM Tris-HCl, 50 mM KCl, 1 mM EDTA, 5 mM MgCl₂, 10% glycerol, pH 8.0). Bs-FtsZ was purified as described (1) with modifications. PMSF (200 µg/mL) and leupeptin (2 µg/mL) were added to the cells in TKM buffer. Cells were disrupted by sonication and centrifuged at 100,000 x g for one hour. The protein in the supernatant was precipitated with 40% ammonium sulphate, resuspended in 50 mM Mes-KOH, 5 mM MgCl₂, 10% glycerol, pH 6.5, and loaded into a 5 mL anion-exchange chromatography HiTrap Q HP column (GE Healthcare). FtsZ was eluted using a 40 minute long 0-1M KCl gradient at 1ml/min. FtsZ was concentrated and subjected to a hydrophobic chromatography with a 1 ml Phenyl HP column (Amersham) in 50mM KH₂PO₄/K₂HPO₄-KOH, 1mM EDTA, 0.8M (NH₄)₂SO₄, pH 7.5, eluted by depletion of (NH₄)₂SO₄ in a 100-0% gradient for 20 minutes at 1ml/min. Finally the protein was subjected to gel-filtration chromatography (Sephacryl S300 26/60 column, GE Healthcare) in 50 mM Tris-HCl, 50mM KCl, 1 mM EDTA, 10% glycerol, pH 7.5, concentrated to < 0.5 mL (about 1mM Bs-FtsZ) and stored at -80°C. Bs-FtsZ preparations contained ~0.1 guanine nucleotide bound per FtsZ, determined by perchloric acid extraction (2). The molecular mass of full length Bs-FtsZ was confirmed by MALDI-TOF mass spectrometry. The Bs-FtsZ concentration was determined spectrophotometrically, after subtracting the nucleotide contribution (2), employing an extinction coefficient 2560 M⁻¹ cm⁻¹ at 280 nm (2 Tyr, 0 Trp residues).

The complete *S. aureus* (Mu50/ATCC 700699) *ftsZ* ORF was amplified with flanking oligos carrying targets for *NdeI* and *BamHI* enzymes, digested, cloned into pET29 and sequenced. The construction was transformed into *E. coli* BL21(DE3)pLys cells, grown in LB medium (1L) with 50ug/mL kanamycin and chloramphenicol and expression induced with 1 mM IPTG (3h at 37 °C). Sa-FtsZ was purified and its molecular mass confirmed as for Bs-FtsZ. It contained ~0.05 guanine nucleotide per FtsZ. The Sa-FtsZ concentration was determined spectrophotometrically, after subtracting the nucleotide contribution (2), employing an extinction coefficient 1960 M⁻¹ cm⁻¹ at 260 nm (14 Phe, 0 Tyr, 0 Trp residues).

FtsZ from *E. coli* was overproduced in transformed *E. coli* BL21(DE3) cells and purified with the Ca²⁺-precipitation and anion-exchange method as described (2), yielding preparations with ~0.8 guanine nucleotide per FtsZ. The concentrations of Ec-FtsZ, Bs-FtsZ and Sa-FtsZ stocks were compared by quantifying their Coomassie stained bands in the same SDS-PAGE gels. Purities of the three different FtsZ are shown by Fig. S6.

Tubulin was purified from bovine brain and microtubules assembled in glycerol containing buffer with 1 mM GTP, pH 6.7, 37 °C, as described (3), employing the scattering and electron microscopy methods described below.

Synthetic compounds. PC190723 (4) was > 99% pure in HPLC analysis. The absorption spectrum of PC in methanol has maxima at 200, 220 and 296 nm and a shoulder at 304 nm. The extinction coefficient at 296 nm is 7300 ± 300 M⁻¹ cm⁻¹ (7085 ± 200 M⁻¹ cm⁻¹ in DMSO).

DFMBA and DFHBA were synthesized following described procedures (5). DFMBA: ^1H RMN (300 MHz, acetone- d^6): 3.89 (s, 3H); 6.98 (td, $J = 9.0, 2.0$ Hz, 1H); 7.14-7.22 (m, 2H); 7.42 (s, 1H). mp = 169.5-170.6 °C. DFMBA was > 99% pure in HPLC-MS analysis. HPLC conditions: MeOH/H₂O-0.1% HCOOH-0.1% NH₄OH, 0-100% for 45 min, 0.5 mL/min, detection at 210/230/254/280 nm for 60 min, t_R : 18.5. m/z 188 [M+H]⁺.

DFHBA: ^1H RMN (300 MHz, acetone- d^6): 6.87 (td, $J = 8.8, 1.8$ Hz, 1H); 6.99-7.07 (m, 1H); 7.26 (s, 1H); 7.48 (s, 1H); 8.85 (s, 1H). mp = 127.0-128.2 °C. DFHBA was > 99% pure in HPLC-MS analysis. HPLC conditions: MeOH/H₂O-0.1 % HCOOH-0.1% NH₄OH, 0-100% for 45 min, 0.5 mL/min, detection at 210/230/254/280 nm for 60 min, t_R : 12.4. m/z 172 [M-H]⁻.

CTPM was synthesized as follows. To a solution of 2-(benzyloxymethyl)-6-chlorothiazolo[5,4-*b*]pyridine (5) (1 g, 3.74 mmol) in distilled CH₂Cl₂ (2 mL), a solution of BBr₃ in DCM (19 mL, 1M) was added dropwise. The mixture was stirred at room temperature for 2 h. After the completion of the reaction, NaHCO₃ (18 mL, sat. solution) was added at 0 °C and the mixture extracted with DCM (3x 40 mL). The organic layers were dried (Na₂SO₄) and evaporated. The resultant solid was purified by column chromatography on silica (Hexane/EtOAc 8:2 to EtOAc) to afford the desired compound in 83% yield. ^1H RMN (300 MHz, CDCl₃): 5.09 (s); 8.21 (d, $J = 2.2$ Hz, 1H); 8.55 (d, $J = 2.2$ Hz). ^{13}C RMN (75 MHz, CDCl₃): 63.6 (CH₂); 129.8 (CH); 130.3 (C); 146.4 (CH); 146.9 (C), 156.3 (C); 176.2 (C). mp = 194.3-195.5 °C. CTPM was > 99% pure in HPLC-MS analysis. HPLC conditions: MeOH/H₂O-0.1 % HCOOH-0.1% NH₄OH, 0-100% for 45 min, 0.5 mL/min, detection at 210/230/254/280 nm for 60 min, t_R : 123.0. m/z 201.0 [M-H]⁺

MBA was from Aldrich.

Monitoring FtsZ assembly with light scattering. FtsZ (10 μM in 0.5 mL filtered buffer, to which ligands were added) was placed in a 10 x 2 mm (excitation path) cell in a photon-counting Horiba-Jovin-Yvon FluoroMax-4 spectrofluorometer thermostated at 25°C. The 350 nm light scattered at 90° (with 0.5 nm excitation and emission band pass), was normalized by the internal reference beam and was recorded in 1 second time frames. The reaction was started by consecutive additions of 10 mM MgCl₂ and guanine nucleotide. The arbitrary scattering units employed through this work are 10⁻⁶ x counts per second (sample) / microAmps (reference).

Electron Microscopy. For negative staining, samples (10-20 μl) were adsorbed to carbon-coated copper electron microscopy grids and stained with 2% uranyl acetate. For cryo-electron microscopy (cryo-EM), samples were applied to grids with holey carbon film (Quantifoil) after glow-discharge and immediately blotted and vitrified using the automatic GATAN cryo-plunge. Micrographs were taken at x40000 magnification in a Jeol 1230 electron microscope operated at 100 kV and equipped with a GATAN liquid nitrogen specimen holder for cryo-EM. Cryo-electron micrographs were taken from the hole areas, where the ice lacks any supporting film underneath, under low dose conditions and different defocus. Micrographs were digitized with a Minolta Dimage Scan Multi Pro scanner at 2400 dpi, corresponding to 0.265 nm per pixel. To measure the thickness of the FtsZ filaments, the images were saved as .PNG files and measured with Image-J. Measurements obtained in pixels were multiplied by 0.265 nm per pixel (6). Cryo-EM images were subsequently low-pass filtered to remove the noise present at high frequencies using EMAN.

FtsZ polymers pelleting. Samples (0.1 mL) were prepared in polycarbonate ultracentrifuge tubes in a thermostat at 25°C. Control samples included one where GTP was substituted with GDP and another lacking MgCl₂. Polymerization was initiated by the addition of nucleotide or of 10 μM FtsZ and typically allowed to proceed for 15 minutes before centrifugation at 386,000 x g (100,000 rpm) for 20 or 80 minutes at 25°C in a TLA-100 rotor with an Optima TLX ultracentrifuge (Beckman). To pellet FtsZ bundles with reduced filament sedimentation, samples were centrifuged at 15,000 x g (20,000 rpm). Supernatants were removed and added one equivalent volume of SDS-PAGE sample buffer. Pellets were carefully resuspended in one volume of sample buffer and one volume buffer added. Pellet and supernatant aliquots from each sample were loaded with a 15 minute electrophoretic shift between them into the same lanes of SDS-12% polyacrylamide gels. Gels were stained with Coomassie blue, scanned and the protein bands quantified using Quantity One software (BioRad).

Screen of solution conditions. The effects of the solution variables on the spontaneous and PC-enhanced assembly of FtsZ (10 μM) were screened with series of small volume sedimentation and electron microscopy tests, complemented with light scattering. Substitution of K by Na reduced polymerization. Bs-FtsZ polymerization was sensitive to the buffer anion. The order of effectiveness was Mes > Hepes > Pipes > Mops ~Bis-Tris (50 mM, pH 6.6). For example, Bs-FtsZ barely assembled in Pipes with GTP (in contrast with Ec-FtsZ), but formed filaments with GMPCPP or bundles upon PC addition.

Binding of PC to FtsZ polymers. Samples (0.2 mL) containing 10 μM FtsZ and different concentrations of PC in Hepes assembly buffer pH 6.8 with 2 mM GTP were centrifuged for 20 min as above. The supernatants were collected and the pellets were resuspended in the same buffer. To measure the concentration of pelleted FtsZ and FtsZ in the supernatant, 5 μl of the samples were separated and applied to a SDS-PAGE gel. Ten micromolar taxol was added as the internal standard to each sample. Both the pellets and the supernatants were then extracted three times with an excess volume of dichloromethane, dried in vacuum, and dissolved in 35 μl of a methanol/water (v/v: 80/20) mixture. PC bound to pelleted polymers and free in the supernatant were determined by HPLC analysis with a C-18 column (Eclipse XDB-C18, 4.6 x 150 mm, 5 μm bead size) eluted with a gradient of 5 mM ammonium acetate to acetonitrile (10% to 90%) in 30 minutes and at a flow rate of 0.5 ml/min.

GTPase. GTP hydrolysis in FtsZ solutions at 25°C was measured from the released inorganic phosphate employing the malachite green method (7). GTPase units are defined as mol of phosphate per mol protein per minute.

Binding of ³H-GTP to FtsZ. Samples (0.2 mL) containing 1 μM FtsZ and 1 μM ³H-GTP (Amersham; diluted into cold GTP to give about 50000 cpm per sample) were prepared in polycarbonate ultracentrifuge tubes at 25°C. Control samples contained an excess of GDP (100 μM). Samples were centrifuged at 386000 x g for 1.5 hours in a TLA100 rotor at 25°C. Samples were carefully divided into a top and a bottom half, an equivalent volume of buffer (100 μl) was added and the free GTP concentration was determined in the protein-depleted top half of tubes, after dilution in 3.8 ml of Beckman ReadySafe solution, employing a LKB Wallac 1219 Rackbeta liquid scintillation counter (PerkinElmer Life Sciences). Bound GTP was determined by difference to the total GTP concentration. In each assay, controls without FtsZ were included, and concentrations were corrected for the small amount of ³H-GTP sedimented in the absence of protein.

REFERENCES

1. Oliva, M.A., Trambaiolo, D., and Löwe, J. (2007) *J. Mol. Biol.* **373**, 1229-1242.
2. Rivas, G., López, A., Mingorance, J., Ferrándiz, M.J., Zorrilla, S., Minton, A.P., Vicente, M., and Andreu, J.M. (2000) *J. Biol. Chem.* **275**, 11740-11749.
3. Andreu, J.M. (2007) *Meth. Mol. Medicine* **137**, 17-28.
4. Haydon, D.J., Stokes, N.R., Ure, R., Galbraith, G., Bennett, J.M., Brown, D.R., Baker, P.J., Barynin, V.V., Rice, D.W., Sedelnikova, S.E., Heal, J.R., Sheridan, J.M., Aiwale, S.T., Chauhan, P.K., Srivastava, A., Taneja, A., Collins, I., Errington, J., and Czaplewski, L.G. (2008) *Science* **321**, 1673-1665.
5. Brown, D.R., Collins, I., Czaplewski, L.G., and Haydon, D.J. (2007) Preparation of substituted benzamides and pyridylamides as antibacterial agents. *PCT Int. Appl.* WO 2007107758 A1 20070927.
6. Huecas, S., Llorca, O., Boskovic, J., Martin-Benito, J., Valpuesta, J.M., and Andreu J.M. (2008) *Biophys. J.* **94**, 1796-1806.
7. Kodama, T., Fukui, K., and Kometani, K. (1986) *J. Biochem.* **99**, 1465-1472.
8. Abal, M., Souto, A.A., Amat-Guerri, F., Acuña, A.U., Andreu, J.M., and Barasoain, I. (2001) *Cell Motil. Cytoskeleton* **49**, 1-15.

TABLE S1. Bs-FtsZ polymorphic assemblies observed under various solution conditions and with PC190723 at 25 °C

POLYMER TYPE (spontaneous)	NUCLEOTIDE, CATION	BUFFER
short filament (few)	GTP/GMPCPP	Hepes 250 mM KCl pH 6.8
Filaments	GTP/GMPCPP, Mg ²⁺	Hepes 50 mM KCl pH 6.8 or pH 7.5 Hepes 250 mM KCl pH 6.8
curved filaments	GMPCPP, Mg ²⁺	Hepes 50 mM KCl pH 6.8
coils ~200 nm Ø	GMPCPP, Mg ²⁺	Hepes 50 mM KCl pH 6.8 Mes 50 mM KCl pH 6.8
toroids ~150 nm Ø	GMPCPP/GTP, Mg ²⁺	Hepes 50 mM KCl pH 6.8

		Mes 50 mM KCl pH 6.8
POLYMER TYPE (with PC190723)		
toroids ~300 nm Ø	GTP	Hepes 50 mM KCl pH 6.8
curved filaments	GTP/GMPCPP	Hepes 250 mM KCl pH 6.8
coils ~200 nm Ø	GTP/GMPCPP	Hepes 250 mM KCl pH 6.8
ribbon and bundle	GTP/GMPCPP, Mg ²⁺	Mes 50 mM KCl, Hepes 50 mM KCl pH 6.8, eventually Hepes 250 mM KCl
helical bundle	GTP, Mg ²⁺	Hepes 50 mM KCl pH 7.5

FIGURE LEGEND

Fig. S1. Polymers formed by Bs-FtsZ (10 µM) in Hepes250 assembly buffer with 2 mM GTP (A), 2 mM GTP plus 20 µM PC (B), 2 mM GTP plus 10 µM MgCl₂ (C), and 2 mM GTP plus 10 mM MgCl₂ and 20 µM PC (D). The bar indicates 200 nm

Fig S2. PC-induced Bs-FtsZ polymers sedimentation in Hepes250 assembly buffer with 10 mM MgCl₂ and GMPCPP (0.1 mM, upper panel) or GTP (2 mM, lower panel). The solid circles are with 20 µM PC, void circles without PC, solid triangles with GMPCP or GDP, void triangles without MgCl₂. The X-axis intercept values were: GTP, 0.0 ± 0.1 µM; GMPCPP, 0.1 ± 0.4 µM.

Fig. S3. Effects of PC on the binding of ³H-GTP (1 µM) to Bs-FtsZ (1 µM) (circles) and Ec-FtsZ (squares) in Hepes50 assembly buffer with 10 mM MgCl₂. The effects of controls with 100 µM GDP added are indicated (triangles).

Fig. S4. A comparison of the effects of PC (20 µM, solid red lines) on the polymerization of FtsZ from susceptible (Bs, Sa) and resistant bacteria (Ec) (dashed lines are without PC). A, Bs-FtsZ. B, Sa-FtsZ. C, Ec-FtsZ. D, Ec-FtsZ with GTP regenerating system (1 unit/mL acetate kinase and 15 mM acetyl phosphate) monitored by light scattering. Conditions: Hepes50 buffer with 10 mM MgCl₂ and 1 mM GTP, 10 µM FtsZ, 25 °C.

Fig. S5. Spindle pole delocalizing effects of taxol on mitotic of A549 human lung carcinoma cells. A and B, no taxol. C and D, 300 nM taxol (24 hour). This figure is only intended to illustrate the analogy, saving systems differences, with the delocalizing effects of PC on the FtsZ ring of *B. subtilis* cells (see Fig. 2B in ref. 4). The bar indicates 10 µm. The microtubules were stained with a monoclonal antibody to alpha-tubulin and a secondary fluoresceinated antibody (green) and DNA with Hoescht 33342. Figure courtesy of I. Barasoain, Centro de Investigaciones Biológicas (see ref. 8 for related results).

Fig. S6. SDS-PAGE of FtsZ preparations. Purities were: Bs-FtsZ 98%, Sa-FtsZ 93% and Ec-FtsZ > 98%, estimated by scanning and quantifying Coomassie blue stained gels. The mobilities of apparent molecular weight markers (KDa) are indicated on the left. Trace contaminants identified by tryptic peptide MALDI-MS/MS fingerprinting in Bs-FtsZ preparations were beta-galactosidase (LacZ) and DnaK from the Ec expression system.

Fig. S1

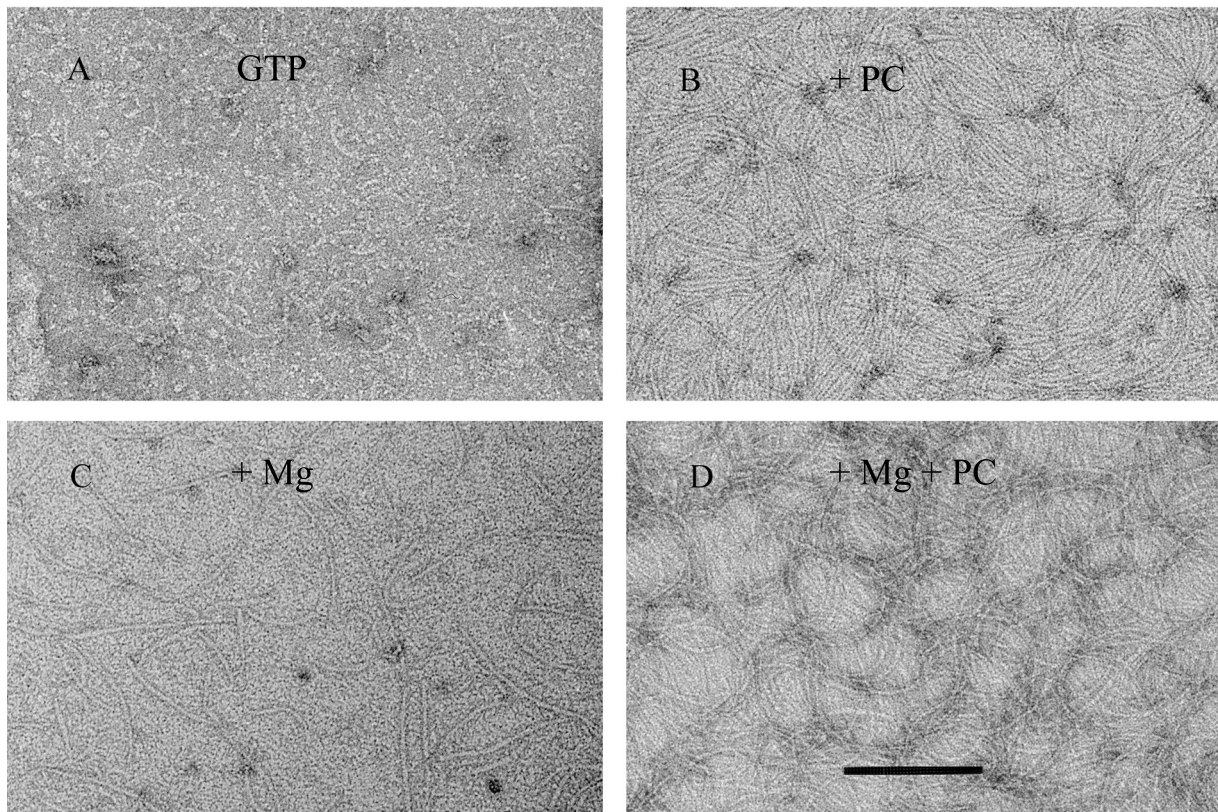


Fig. S2

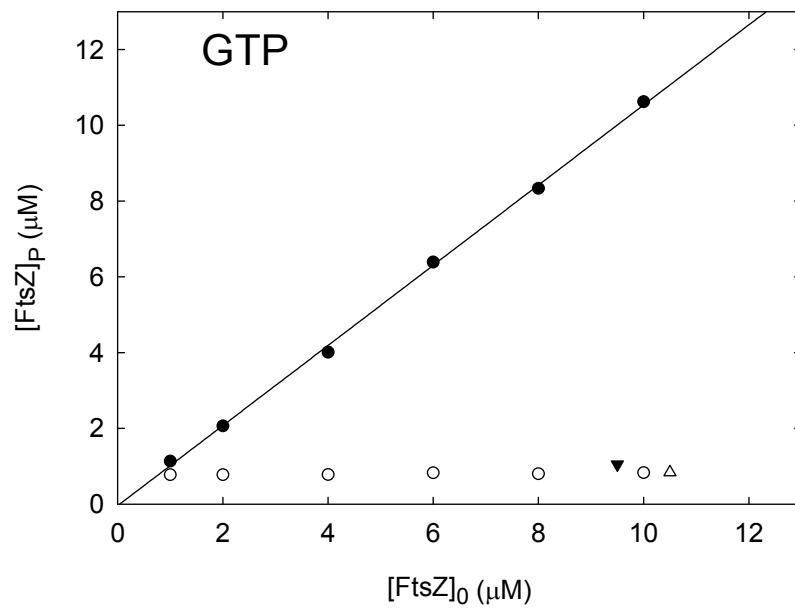
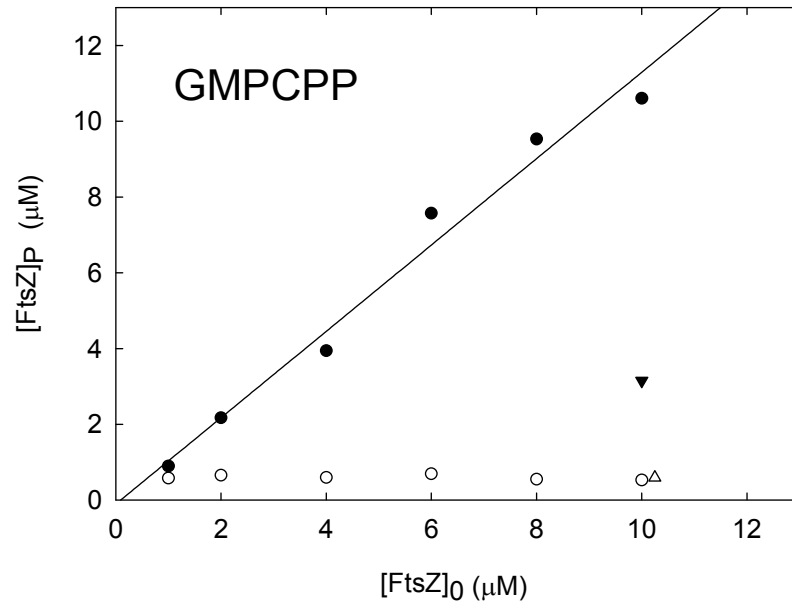
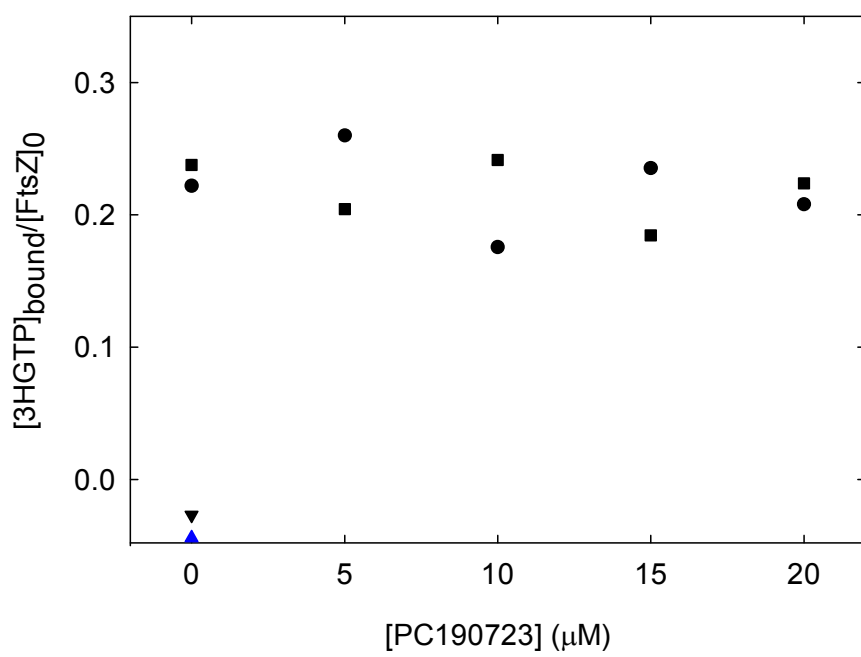


Fig. S3



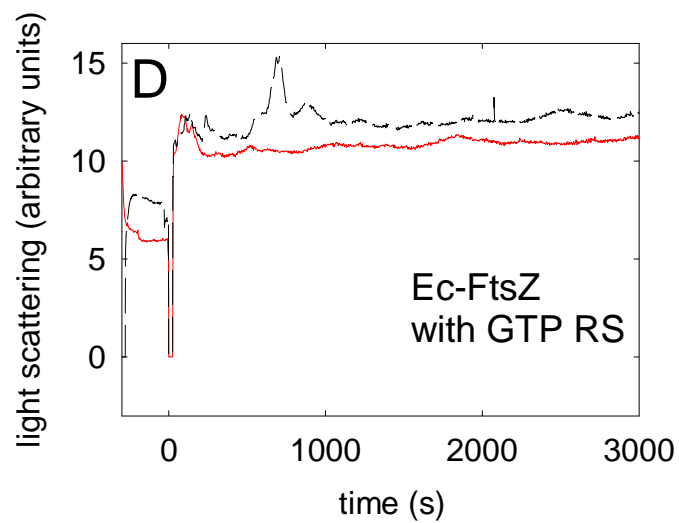
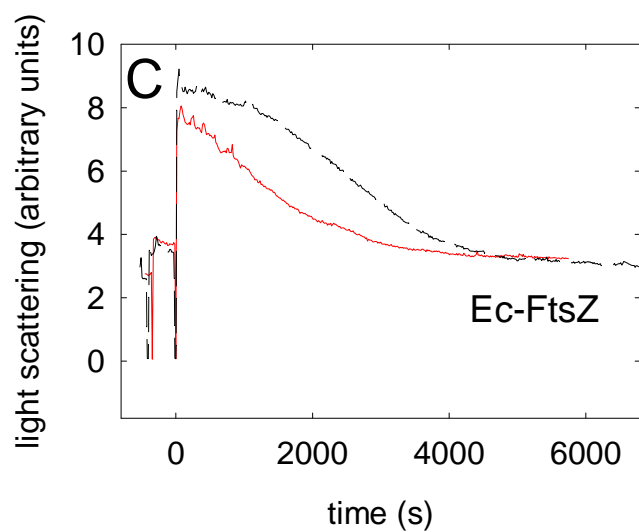
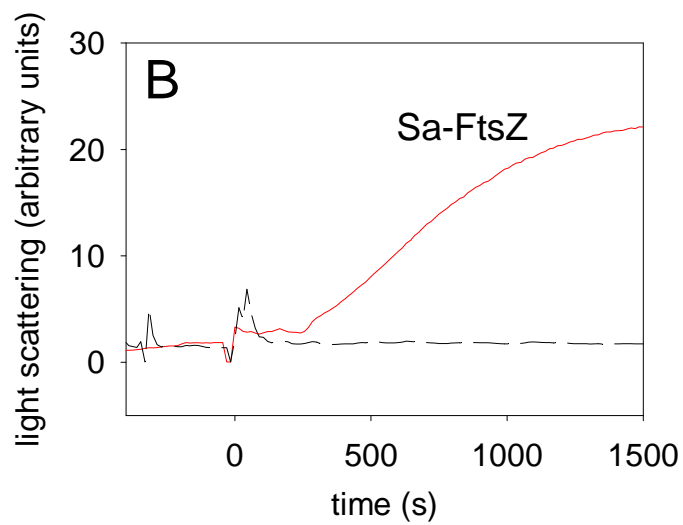
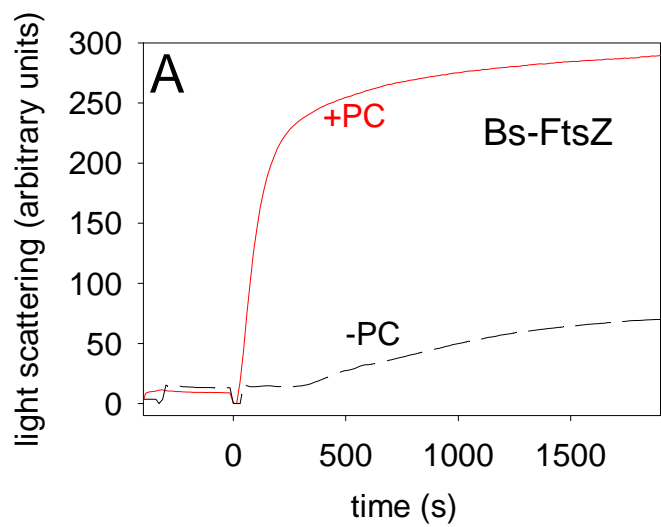
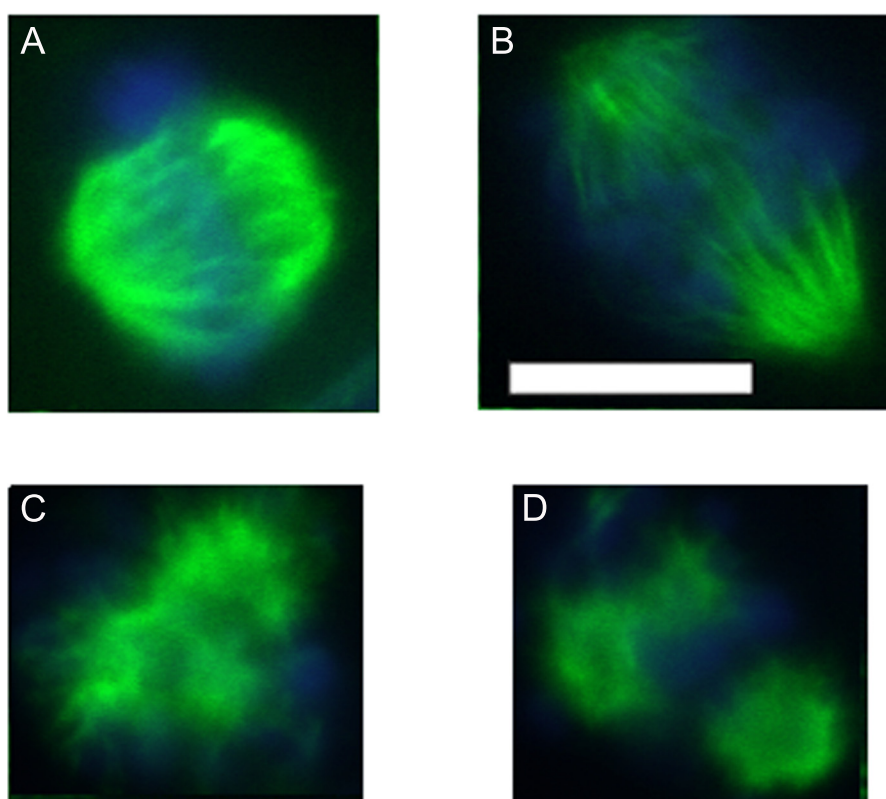
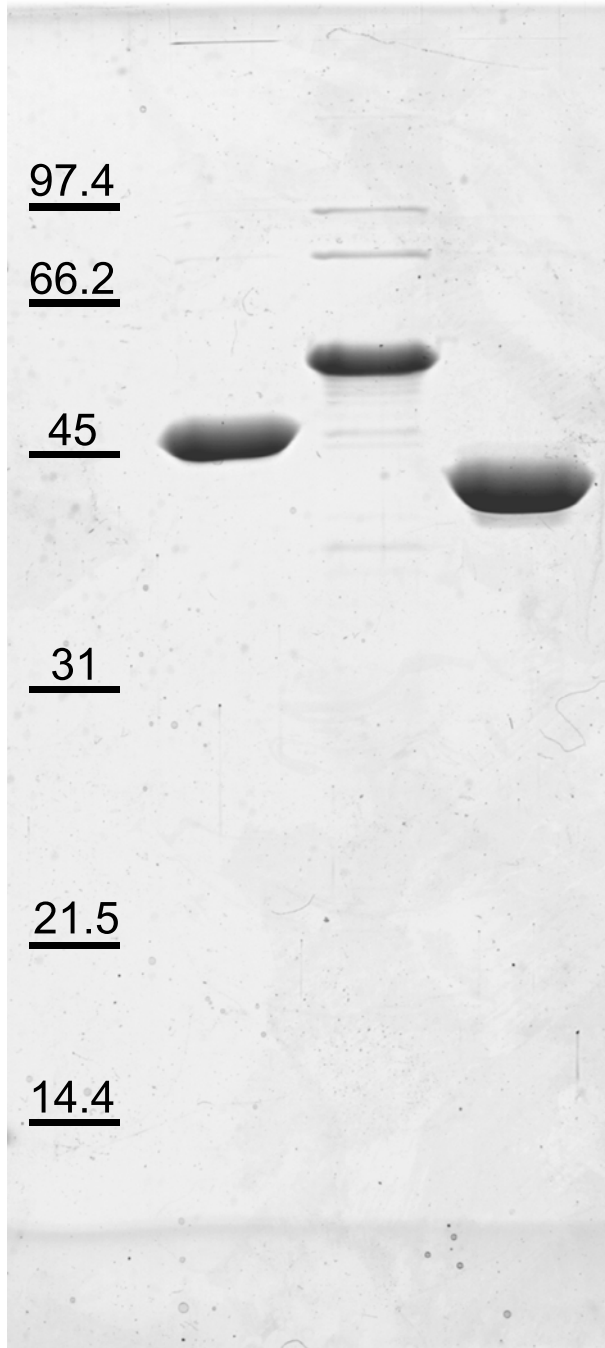


Fig. S5



Bs Sa Ec



The Antibacterial Cell Division Inhibitor PC190723 Is an FtsZ Polymer-stabilizing Agent That Induces Filament Assembly and Condensation

José M. Andreu, Claudia Schaffner-Barbero, Sonia Huecas, Dulce Alonso, María L. Lopez-Rodriguez, Laura B. Ruiz-Avila, Rafael Núñez-Ramírez, Oscar Llorca and Antonio J. Martín-Galiano

J. Biol. Chem. 2010, 285:14239-14246.

doi: 10.1074/jbc.M109.094722 originally published online March 8, 2010

Access the most updated version of this article at doi: [10.1074/jbc.M109.094722](https://doi.org/10.1074/jbc.M109.094722)

Alerts:

- [When this article is cited](#)
- [When a correction for this article is posted](#)

[Click here](#) to choose from all of JBC's e-mail alerts

Supplemental material:

<http://www.jbc.org/content/suppl/2010/03/08/M109.094722.DC1>

This article cites 51 references, 18 of which can be accessed free at

<http://www.jbc.org/content/285/19/14239.full.html#ref-list-1>